Reverse-time migration: Comparing three numerical solvers

Alejandro Cabrales-Vargas

ABSTRACT

I compare the results of three numerical schemes for seismic modeling and reverse-time migration: the rapid expansion method, the Lax-Wendroff method, and the pseudo-analytical method. The rapid expansion method uses coarse time steps without developing instabilities, but it can present frequency dispersion when using coarse grids. Moreover, its implementation is difficult. The Lax-Wendroff method can avoid such limitations at the expense of time step refinement, thereby more Laplacian computations. Both methods allow the representation of the space derivatives either in the spatial domain (finite differences method) or in the Fourier domain (pseudospectral method). The pseudo-analytical method offers an accurate solution and easy implementation, but it is restricted to the Fourier domain.

INTRODUCTION

During the last decade, reverse-time migration (RTM) has been adopted as the ultimate solution for imaging very complex geology. Although geoscientists have known about RTM potential for 30 years (Baysal et al., 1983; Kosloff and Baysal, 1983; McMechan, 1983; Gazdag and Carrizo, 1986), it only recently became affordable. However, it is still computationally intensive, so the search of cheaper and more accurate implementations of the two-way wave equation continues. This fact is particularly crucial when thinking of forward and reverse-time propagation as the main engines behind state-of-the-art iterative solutions, such as least-squares migration and full-waveform inversion.

Traditionally, second-order time derivatives in the wave equation have been approximated using second-order finite differences (Baysal et al., 1983; Kosloff and Baysal, 1983; Gazdag and Carrizo, 1986; Dablain, 1986). This scheme is easy to implement and conceptually simple. However, for the sake of stability the Courant-Friedrichs-Lewy (CFL) criterion usually requires time step refinements (Dablain, 1986). Computations increase in proportion to the interpolation factor. Making the grid coarser solves the problem, but reducing the maximum frequency that can be handled without dispersion. The balance between stability and numerical dispersion for the second-order approximation is stringent because it originates from a Taylor series expansion with only two terms, thus assuming small time steps in relation to the grid size.

One obvious solution to relax the stability threshold is to implement better approximations that tolerate less refinements of time steps. In the limit, we may want an approximation that does not require refinement altogether. Incorporating more terms to the approximation in principle achieves this goal, but high-order times derivatives appear. Fortunately, we can compute such time derivatives by means of second-order spatial derivatives according to the wave equation. The Lax-Wendroff method (LWM) (Dablain, 1986; Chen, 2007; Zhang et al., 2007; Pestana and Stoffa, 2010) makes use of this technique approximating the fourth-order time derivative by cascading the Laplacian operator (multiplied by the medium velocity) twice. On the contrary, the rapid expansion method (REM) (Tal-Ezer et al., 1987; Kosloff et al., 1989; Jastram and Behle, 1991; Tessmer, 2011; Stoffa and Pestana, 2009; Pestana and Stoffa, 2010; Araujo et al., 2014) takes a further step, using an expansion in Chebyshev polynomials and cascading as many terms as required to achieve convergence. The number of terms is tied to the time step, so that any time step can be used when enough terms are incorporated. The spatial derivatives in LWM and REM can be computed using finite differences (Jastram and Behle, 1991) or the pseudospectral method (Tal-Ezer et al., 1987; Kosloff et al., 1989; Jastram and Behle, 1991; Tessmer, 2011; Stoffa and Pestana, 2009; Pestana and Stoffa, 2010; Araujo et al., 2014)

A relatively new solution is the pseudo-analytical method (PAM), originally proposed by Etgen and Brandsberg-Dahl (2009), and later modified by dos Santos and Pestana (2012). The original propose uses so-called *pseudo-Laplacians* to propagate constant-velocity wavefields, which are subsequently interpolated to incorporate velocity variations. In their modified version, dos Santos and Pestana (2012) compute a *pseudo-Laplacian* that "pivots" around a reference constant velocity (usually the minimum or the maximum in the model), and introduces velocity variations by means of perturbations of such reference velocity. The advantage of this method is that it is almost as simple as the second-order time marching scheme, but keeping stability at coarser time steps, and almost free of frequency dispersion. It is considerably easier to implement than the REM. One drawback is that it only can be implemented in the Fourier domain.

In the following section I briefly present the theory of the three methods. Next, I compare their performance in modeling and migration applied to a synthetic, normal fault model. Finally, I present the conclusions of this report.

LAX-WENDROFF METHOD

Given an exploding source, $\mathbf{f}(\mathbf{x},t)$, ignited in an acoustic, constant density medium, the propagation wavefield satisfies the 2D acoustic wave equation:

$$\frac{\partial^2 \mathbf{u}}{\partial t^2} = -\mathbf{L}^2\mathbf{u} + \mathbf{f}, \tag{1}$$

where $\mathbf{u}(\mathbf{x},t)$ is the displacement field, and $-\mathbf{L}^2 = v(x,z)^2\nabla^2$ constitutes the

Laplacian scaled by the squared of the interval velocity. The corresponding expressions in the physical domain and in the Fourier domain are, respectively,

$$-\mathbf{L}^2 = v(x,z)^2\left(\frac{\partial^2}{\partial x^2}+\frac{\partial^2}{\partial z^2}\right), \tag{2}$$

and

$$-\mathbf{L}^2 = -v(x,z)^2(\mathbf{k_x}^2+\mathbf{k_z}^2), \tag{3}$$

where $\mathbf{k_x}$ and $\mathbf{k_z}$ are the spatial wavenumbers. Note that in the last equation we mixed physical domain variables with Fourier domain variables. While formally violating the assumption of constant velocity, in practice this artifice eases maneuvering the equations, and the conclusions extracted are fundamentally correct.

The solution the homogeneous version of Equation 1 (source term equals to zero) subject to non-zero initial conditions is

$$\frac{\partial^2\mathbf{u}}{\partial t^2} = -\mathbf{L}^2\mathbf{u}, \tag{4}$$

$$\mathbf{u}(t=0) = \mathbf{u}(0), \frac{\partial\mathbf{u}(t=0)}{\partial t} = \dot{\mathbf{u}}(0), \tag{5}$$

where $\mathbf{u}(0)$ and $\dot{\mathbf{u}}(0)$ constitute the initial displacement field and its first time derivative, respectively. Thus, the formal solution of Equation 4 for forward propagation in time is

$$\mathbf{u}(t) = \mathbf{u}(0)\cos(\mathbf{L}t) + \dot{\mathbf{u}}(0)\frac{\sin(\mathbf{L}t)}{\mathbf{L}}. \tag{6}$$

Likewise, the solution for backward propagation in time is

$$\mathbf{u}(-t) = \mathbf{u}(0)\cos(\mathbf{L}t) - \dot{\mathbf{u}}(0)\frac{\sin(\mathbf{L}t)}{\mathbf{L}}. \tag{7}$$

Adding Equation 6 to Equation 7 eliminates the derivative of the initial displacement:

$$\mathbf{u}(t) + \mathbf{u}(-t) = 2\cos(\mathbf{L}t)\mathbf{u}(0). \tag{8}$$

Using Taylor series expansion to approximate the cosine operator:

$$\mathbf{u}(t) + \mathbf{u}(-t) = \left[2 + t^2\mathbf{L}^2 + \frac{t^4}{12}\mathbf{L}^4 + ...\right]\mathbf{u}(0). \tag{9}$$

Finally, replacing the reference time, $t = 0$, for any time, t, and propagating the solution in time steps, Δt, we obtain:

$$\mathbf{u}(t+\Delta t) + \mathbf{u}(t-\Delta t) = \left[2 + \Delta t^2\mathbf{L}^2 + \frac{\Delta t^4}{12}\mathbf{L}^4\right]\mathbf{u}(t). \tag{10}$$

In Equation 10 I have truncated the series beyond the fourth-order term, therefore it constitutes a fourth-order approximation of the second derivative in time. Equation 10 is the classical solution of the acoustic wave equation using the Law-Wendroff method (Dablain, 1986; Chen, 2007). Operator $\mathbf{L}^2$ can be implemented in the Fourier domain (pseudospectral) or with finite differences (Equations 2 and 3, respectively).

RAPID EXPANSION METHOD: ONE-STEP APPROACH

The formal solution of the acoustic wave equation (Equation 1) subject to zero initial conditions is (Tal-Ezer et al., 1987; Kosloff et al., 1989)

$$\mathbf{u}(\mathbf{x},t) = \int_0^t \frac{\sin\left(\mathbf{L}(t-\tau)\right)}{\mathbf{L}}\mathbf{f}(\mathbf{x},\tau)d\tau. \tag{11}$$

The numerical approximation to Equation 11 when the source is separable, $\mathbf{f}(\mathbf{x},t) = \mathbf{g}(\mathbf{x})s(t)$, is

$$\mathbf{u}(\mathbf{x},t) = 2\sum_{k=0}^{M} b_{2k+1}(t)\frac{R}{i\mathbf{L}}Q_{2k+1}\left(\frac{i\mathbf{L}}{R}\right)\mathbf{g}(\mathbf{x}), \tag{12}$$

where Q_k are modified Chebyshev polynomials of first kind and order k (the coefficients are positive, whereas in original polynomials they have alternating signs), and R is a scalar larger than the largest eigenvalue in $\mathbf{L}$, therefore keeping the norm of the polynomials argument less than 1. Function $\mathbf{g}(\mathbf{x})$ is an impulse spike in space that indicates the position of the source, and

$$b_k(t) = \frac{1}{R}\int_0^t J_k(\tau R)s(t-\tau)d\tau, \tag{13}$$

where J_k are Bessel functions of first kind and order k, and $s(t)$ is the source signature. Note that only odd k values are required in the series. The value of R can be calculated as

$$R = \frac{1.1\pi V_{max}\sqrt{2}}{min(\Delta x, \Delta z)}. \tag{14}$$

Summation 12 converges for $M > Rt_{max}$ expansion terms. Given recording times of typical seismic surveys, subsurface velocities, and grid sizes, the value of M would be the order of thousands. This fact discourages the explicit computation of the Chebyshev polynomials coefficients. Instead, the polynomials are recursively calculated for the source position function $\mathbf{g}(\mathbf{x})$, initializing with

$$\frac{R}{i\mathbf{L}}Q_1\left(\frac{i\mathbf{L}}{R}\right)\mathbf{g}(\mathbf{x}) = \mathbf{g}(\mathbf{x}), \tag{15}$$

$$\frac{R}{i\mathbf{L}}Q_3\left(\frac{i\mathbf{L}}{R}\right)\mathbf{g}(\mathbf{x}) = 3\mathbf{g}(\mathbf{x}) - 4\left(\frac{\mathbf{L}}{R}\right)^2\mathbf{g}(\mathbf{x}), \tag{16}$$

and calculating successive terms according to

$$\frac{R}{i\mathbf{L}}Q_{2k+1}\left(\frac{i\mathbf{L}}{R}\right)\mathbf{g}(\mathbf{x}) = 2\left[1-2\left(\frac{\mathbf{L}}{R}\right)^2\right]\frac{R}{i\mathbf{L}}Q_{2k-1}\left(\frac{i\mathbf{L}}{R}\right)\mathbf{g}(\mathbf{x})-\frac{R}{i\mathbf{L}}Q_{2k-3}\left(\frac{i\mathbf{L}}{R}\right)\mathbf{g}(\mathbf{x}). \quad (17)$$

The factor $\frac{R}{i\mathbf{L}}$ makes the odd terms of the series contain only even powers of $\frac{i\mathbf{L}}{R}$, yielding flipping signs instead of imaginary numbers.

The computation of the $b_k(t)$ coefficients is time consuming. Fortunately, they are independent of the source position, which means they are computated once for all the shots in a survey, or everytime the source signature significantly varies with position.

As mentioned before, one-step REM approach assumes separability of the source in two independent time and space functions. Such assumption stands for forward propagation of the source wavefield, but breaks down for backward propagation of the receiver wavefield. We can use the recursive implementation of the REM for this case.

RAPID EXPANSION METHOD: RECURSIVE APPROACH

Equation 8 can be approximated by expanding the cosine operator with Chebyshev polynomials:

$$\mathbf{u}(t) + \mathbf{u}(-t) = \sum_{k=0}^{M/2} C_{2k}J_{2k}(Rt)Q_{2k}\left(\frac{i\mathbf{L}}{R}\right)\mathbf{u}(0), \quad (18)$$

where coefficients $C_0 = 1$, and $C_k = 2$ for $k > 0$. The main differences between Equations 12 and 18 are the use of the Bessel functions instead of the b_k coefficients, and the even terms in the summation. The computation can be performed in a single step as shown before. Alternatively (Pestana and Stoffa, 2010; Tessmer, 2011), substituting smaller time steps, Δt, for the total time, t, and an arbitrary time, t, for the reference time, t =0, yields

$$\mathbf{u}(t + \Delta t) + \mathbf{u}(t - \Delta t) = \sum_{k=0}^{M} C_{2k}J_{2k}(R\Delta t)Q_{2k}\left(\frac{i\mathbf{L}}{R}\right)\mathbf{u}(t), \quad (19)$$

which can be solved recursively in time. The initial conditions are injected at each time step. The number of terms required to ensure convergence is $M > R\Delta t$, which is usually less than 20. Therefore, the explicit computation of the Chebyshev polynomials coefficients becomes affordable in recursive REM.

Now we re-order terms of Equation 19 in factors of $\left(\frac{\mathbf{L}}{R}\right)^2$:

$$\mathbf{u}(t + \Delta t) + \mathbf{u}(t - \Delta t) = \sum_{k=0}^{M} A_{2k}\left[\frac{i\mathbf{L}}{R}\right]^{2k}\mathbf{u}(t), \quad (20)$$

where

$$A_k = \sum_{l=k}^{M} C_l J_l(R\Delta t) q_{k,l} \tag{21}$$

and $q_{k,l}$ represents the l coefficient of the Chebyshev polynomial of order k.

Notice that Equation 20 represents a polynomial expansion in even powers of the Laplacian operator. Moreover, if we set $R = 1$, and instead of using Equation 21 we define coefficients A_k as

$$A_0 = 2;\ A_2 = 1;\ A_4 = \frac{1}{12};\ A_k = 0\ \forall\ k > 4, \tag{22}$$

we obtain the representation of the LWM (Equation 10).

PSEUDO-ANALYTICAL METHOD

Following the variant of the PAM proposed by dos Santos and Pestana (2012), we can use the time step marching version of Equation 8,

$$\mathbf{u}(t+\Delta t) + \mathbf{u}(t-\Delta t) = 2\cos\left(\mathbf{L}_0\Delta t\right)\mathbf{u}(t). \tag{23}$$

Here I substitute the operator $\mathbf{L}_0$ for $\mathbf{L}$ to indicate the use of a constant reference velocity, usually defined as the minimum or maximum velocity in the model (dos Santos and Pestana, 2012). The cosine term is recast using the well known trigonometric identity, $\cos(2\theta) = 1 - 2\sin^2(\theta)$, so we obtain

$$\mathbf{u}(t+\Delta t) - 2\mathbf{u}(t) + \mathbf{u}(t-\Delta t) = -2\sin^2\left(\frac{\mathbf{L}_0\Delta t}{2}\right)\mathbf{u}(t). \tag{24}$$

Multiplying and dividing by the appropriate terms, the sine function becomes a sinc function [$\mathrm{sinc}(\theta) = \frac{\sin(\theta)}{\theta}$]:

$$\mathbf{u}(t+\Delta t) - 2\mathbf{u}(t) + \mathbf{u}(t-\Delta t) = -\Delta t^2\mathbf{L}_0^2\mathrm{sinc}^2\left(\frac{\mathbf{L}_0\Delta t}{2}\right)\mathbf{u}(t). \tag{25}$$

In the limit as $\Delta t \to 0$, Equation 25 becomes the constant-velocity, second-order approximation, of the wave equation. The advantage of this scheme is the compensation for frequency-dispersion-related numerical errors (Etgen and Brandsberg-Dahl, 2009), otherwise present when using conventional second-order approximation.

The extension to variable velocity is performed by defining an auxiliary wavefield,

$$\mathbf{p}(\mathbf{x}, t) = \alpha(\mathbf{x})\mathbf{u}(\mathbf{x}, t), \tag{26}$$

where $\alpha(\mathbf{x}) = 1 - \frac{v_0^2}{v(\mathbf{x})^2}$ incorporates the velocity variation as a perturbation of the reference velocity, v_0. This auxiliary wavefield becomes a source term in the acoustic wave equation:

$$\frac{\partial^2\mathbf{u}}{\partial t^2} = -\mathbf{L}_0^2\mathbf{u} + \frac{\partial^2\mathbf{p}}{\partial t^2}. \tag{27}$$

Equation 27 becomes homogeneous by introducing another auxiliary field,

$$\mathbf{u}(\mathbf{x},t) = \mathbf{w}(\mathbf{x},t) + \mathbf{p}(\mathbf{x},t), \tag{28}$$

thus obtaining

$$\frac{\partial^2 \mathbf{w}}{\partial t^2} = -\mathbf{L}_0^2(\mathbf{w}+\mathbf{p}). \tag{29}$$

Finally, we apply the expression for the pseudo-analytical method (Equation 25), to obtain

$$\mathbf{w}(t+\Delta t) - 2\mathbf{w}(t) + \mathbf{w}(t-\Delta t) = -\Delta t^2 \mathbf{L}_0^2 \text{sinc}^2\left(\frac{\mathbf{L}_0 \Delta t}{2}\right)(\mathbf{w}(t)+\mathbf{p}(t)). \tag{30}$$

Equation 30 can be solved for wavefield $\mathbf{w}(\mathbf{x},t)$ like in the constant-velocity case. Function $\alpha(\mathbf{x},t)$ is precomputed, then $\mathbf{p}(\mathbf{x},t)$ is calculated to initialize the recursion in time. The original wavefield is recovered as $\mathbf{u}(\mathbf{x},t) = \mathbf{w}(\mathbf{x},t)/(1-\alpha(\mathbf{x},t))$.

METHODOLOGY AND IMPLEMENTATION

I test the methods discussed in this report modeling and migrating a simple two-bed, normal fault model of the subsurface. The shallow bed has a velocity gradient ranging from 2000 to 2500m/s approximately, and the deep bed has a constant velocity of 5000m/s (Figure 1). Despite its conspicuous structural simplicity, the velocity contrast is strong and the fault dip is about 60°, therefore making the analysis simple in rather challenging conditions. The gridsize is $\Delta x = 12.5$m and $\Delta z = 10$m, covering an extension of 4500m (The model begins at -500m). Therefore, I should be able to model frequencies up to 80Hz (based on the pseudospectral method). The dataset consists of 36 shots equally spaced every 100m. Each shot has 361 receivers spaced every 12.5m, which means that each one covers the model extension.

In order to make fair comparisons with the PAM, I prepared the LWM and the REM tests using the pseudospectral method. All the methods employ tapering boundary conditions (Cerjan et al., 1985). In the migrations tests I use wavefield separation in the imaging condition according to Liu et al. (2011).

In the modeling and RTM tests I employed two different Ricker wavelets as input source: a) dominant frequency of 15Hz and maximum frequency of 50Hz; b) dominant frequency of 50Hz, maximum frequency slightly above 80Hz (the maximum frequency theoretically handled).

For the implementation of the REM, I employed the one-step solution to compute the source wavefield (Equation 12), and the recursive solution for the receiver wavefield (Equation 19).

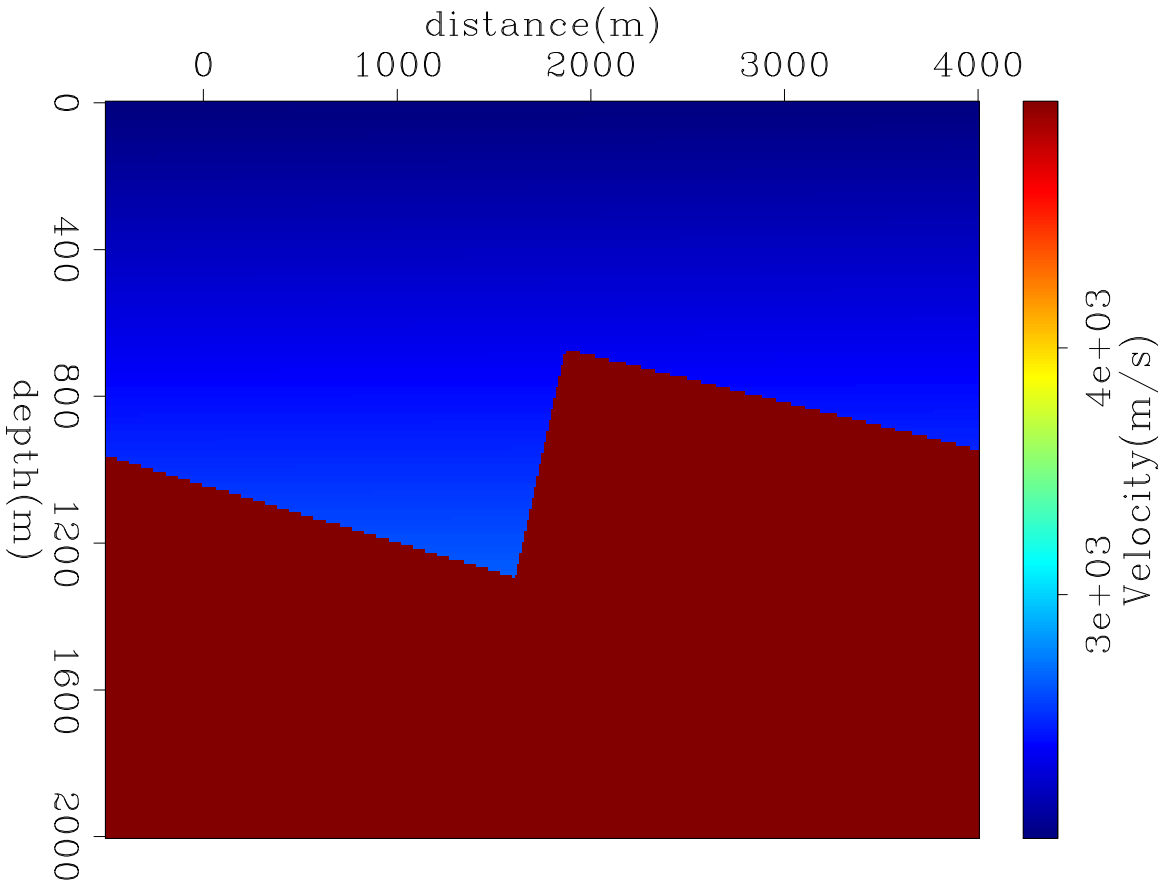

Figure 1: Normal-fault velocity model [**NR**]

NUMERICAL RESULTS

Figure 2 shows the results of the modeling tests with the source wavelet a) in one time frame. We observe the reflection and transmision waves corresponding to the dipping velocity contact between positions 500m and 1800m, and between $1 - 1.6$ km. The diffraction originates at the cusp of the footwall block, partially reflecting back to the 2000m/s layer, whereas the other part transmits through the 5000m/s layer. The rest of the events correspond to attenuated waves that wrapped around the taper boundaries. Such events are mostly present in the Lax-Wendroff and the pseudo-analytical modeling tests, which are virtually identical. In the case of the rapid expansion method such artifacts were highly attenuated. I applied the same boundary conditions in the three methods, but while in Lax-Wendroof and pseudo-analytical methods the tapering is applied to the wavefields every time step, in the rapid expansion method such taper is applied to every Chebyshev polynomial evaluation in Equation 12, before multiplying by the $b_k(t)$ coefficients.

Figures 3 show the results of the tests using the source wavelet b), where the transmitted and reflected events contain higher frequency as expected. In this case we observe that the pseudo-analytical method begins to develop frequency dispersion. Notwithstanding that the stability condition is enforced, small frequency components beyond the theoretically maximum frequency are enough to cause such dispersion. Note the absence of this phenomenon in the Lax-Wendroff and the rapid expansion frames.

I finally present migration tests in Figures 4 and 5 using the source a) and b), respectively, to compute the corresponding source wavefields. It is interesting to notice the presence of low-wavenumber migration artifacts in the case of the Lax-Wendroff method and the rapid expansion method. They seem to be mostly related to the presence of the shap lateral velocity contrast introduced by the normal fault, and can constitute remnants of the RTM typical low-wavenumber numerical noise. Such noise obscures part of the fault plane. There are also high-wavenumber artifacts, very likely related to source undersampling. Both types of numerical artifacts are almost absent in the pseudo-analytical test, so the fault plane is nicely imaged. Moreover, the frequency dispersion observed when going to higher source frequencies is not harming the migrated image. The high reduction of high-wavenumber undersampling artifacts can be explained by the use of the sinc function of the pseudo-Laplacian operator, which is better behaved in the vicinity of the Nyquist wavenumbers. In the case of the reduction of low-wavenumber artifacts, one possible explanation is the computation of the Laplacian entirely in the reference velocity framework. As previously seen, only after such stage the velocity variation is introduced by means of the perturbation α.

CONCLUSIONS

In this report I compare three methods to perform modeling and reverse-time migration: the rapid expansion method, the pseudo-analytical method, and the Lax-

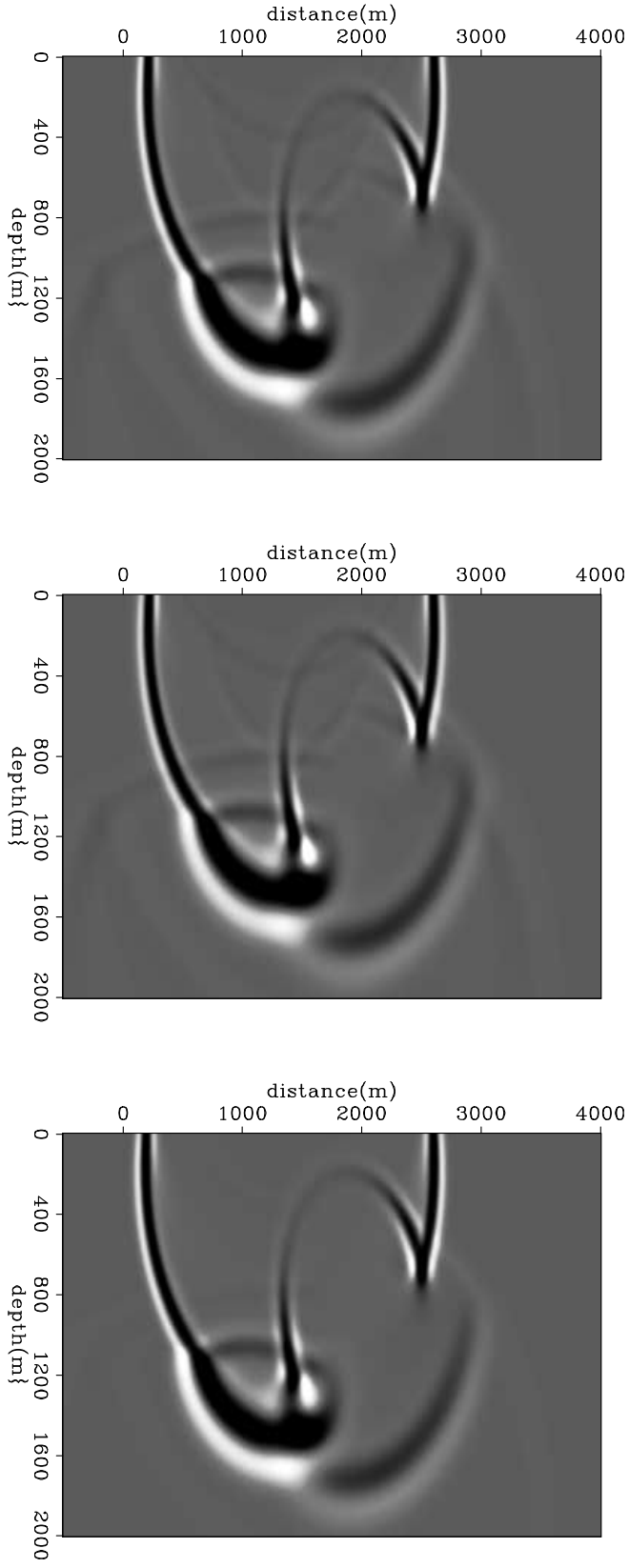

Figure 2: Single-source wavefront propagation using 15Hz Ricker wavelet. *Top*: Lax-Wendroff method; *Middle*: Pseudo-analytical method; *Bottom*: Rapid Expansion method [**CR**]

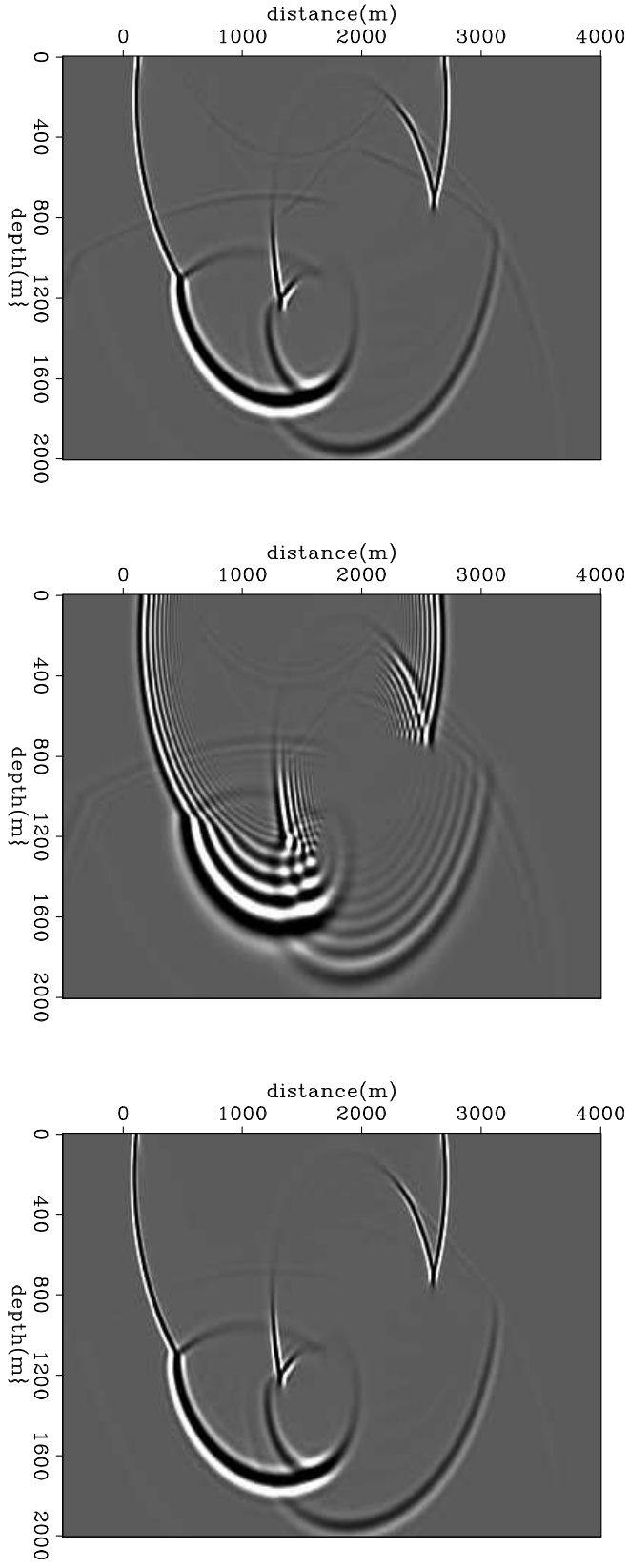

Figure 3: Single-source wavefront propagation using 50Hz Ricker wavelet. *Top*: Lax-Wendroff method; *Middle*: Pseudo-analytical method; *Bottom*: Rapid Expansion method [**CR**]

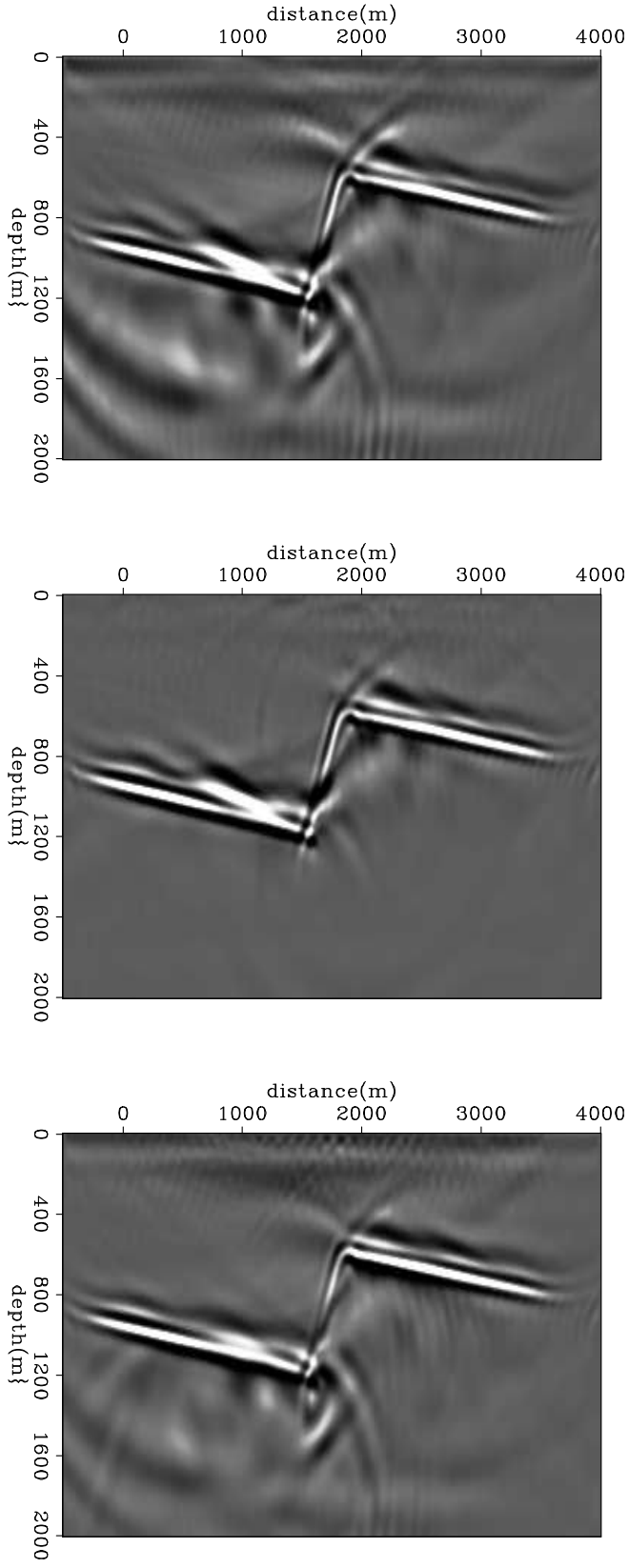

Figure 4: Reverse-time migration stack images using 15Hz Ricker wavelet. *Top*: Lax-Wendroff method; *Middle*: Pseudo-analytical method; *Bottom*: Rapid Expansion method [**CR**]

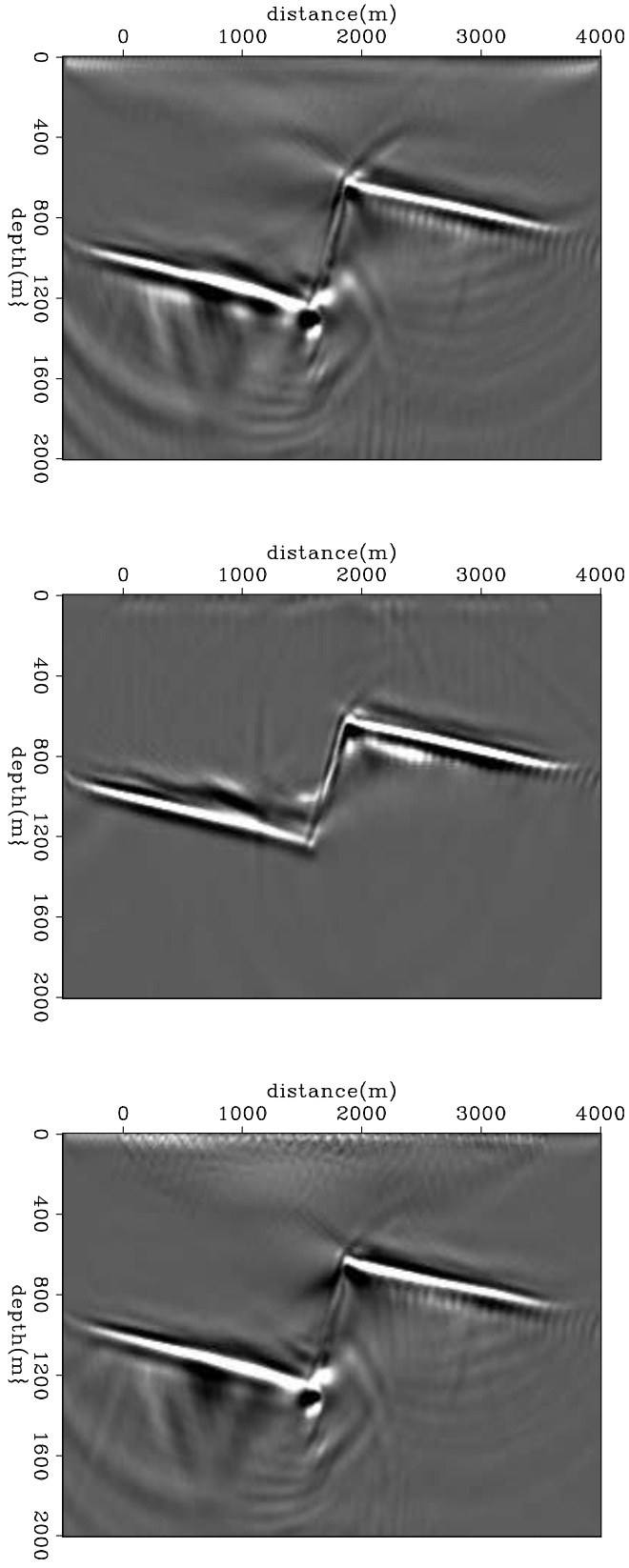

Figure 5: Reverse-time migration stack images using 50Hz Ricker wavelet. *Top*: Lax-Wendroff method; *Middle*: Pseudo-analytical method; *Bottom*: Rapid Expansion method [**CR**]

Wendroff method. I test their performance on a normal fault model of the subsurface, with high velocity contrast.

The rapid expansion method offers stable solutions at arbitrary time steps, but it is cumbersome to code, and requires time functions dependent of Bessel functions that have to be precomputed, more than once in case of spatially-variable source signatures, therefore careful optimization strategies should be implemented to make the method fully efficient. Also, it is constrained to frequency dispersion bounds, which can limit its applicability for arbitrary time steps. The Lax-Wendroff method is an attractive alternative easier to implement, and as the rapid expansion method, it offers the flexibility to solve the Laplacian with finite differences. Nevertheless, the tests show that some low-frequency noise and aliasing noise can be present in both methods. The pseudo-analytical method, in the contrary, although is limited to the Fourier domain for the computation of the pseudo-Laplacian, succeeds in constructing a clean and accurate image, in spite of the frequency dispersion of the source wavefield. The better approximation around the Nyquist wavenumbers, and the computation of the pseudo-Laplacian using the constant reference velocity, can explain the reduction of high frequency noise, while the computation of pseudo-Laplacians using constant velocity can explain the reduction of low-frequency artifacts. More experiments are required to shed more light upon this behavior.

ACKNOWLEDGMENTS

I wish to thank Petroleos Mexicanos for the financial support, and the SEP sponsors and crew. Special thanks to Musa Maharramov, who suggested the comparisons presented in this report, and to Reynam Pestana, who kindly helped me clarify many issues about the rapid expansion method.

REFERENCES

Araujo, E., R. Pestana, and A. dos Santos, 2014, Symplectic scheme and the Poynting vector in reverse-time migration: Geophysics, **79**, no. 5, S163–S172.

Baysal, E., D. Kosloff, and J. Sherwood, 1983, Reverse time migration: Geophysics, **48**, 1514–1524.

Cerjan, C., D. Kosloff, R. Kosloff, and M. Reshef, 1985, A nonreflecting boundary condition for discrete acoustic and elastic wave equations: Geophysics, **50**, 705–708.

Chen, J., 2007, High-order time discretizations in seismic modeling: Geophysics, **72**, no. 5, SM115–SM122.

Dablain, M., 1986, The application of high-order differencing to the scalar wave equation: Geophysics, **51**, 54–66.

dos Santos, A. and R. Pestana, 2012, A pseudo-analytical method to solve the acoustic wave equation for modeling and RTM: SEG Technical Program Expanded Abstracts, 1–5.

Etgen, J. and S. Brandsberg-Dahl, 2009, The pseudo-analytical method: Application of pseudo-Laplacians to acoustic and acoustic anisotropic wave propagation: SEG Technical Program Expanded Abstracts, 2552–2556.

Gazdag, J. and E. Carrizo, 1986, On reverse-time migration: Geophysical Prospecting, **34**, 822–832.

Jastram, C. and A. Behle, 1991, Elastic modeling by finite difference and the rapid expansion method (REM): SEG Technical Program Expanded Abstracts, 1573–1576.

Kosloff, D. and E. Baysal, 1983, Migration with the full acoustic wave equation: Geophysics, **48**, 677–687.

Kosloff, D., A. Filho, E. Tessmer, and A. Behle, 1989, Numerical solution of the acoustic and elastic wave equation by a new rapid expansion method: Geophysical Prospecting, **37**, 383–394.

Liu, F., Z. Guanquan, S. Morton, and J. Leveille, 2011, An effective imaging condition for reverse-time migration using wavefield decomposition: Geophysics, **76**, no. 1, S29–S39.

McMechan, G., 1983, Migration by extrapolation of time-dependent boundary values: Geophysical Prospecting, **31**, 413–420.

Pestana, R. and P. Stoffa, 2010, Time evolution of the wave equation using rapid expansion method: Geophysics, **75**, no. 4, T121–T131.

Stoffa, P. and R. Pestana, 2009, Numerical solution of the acoustic wave equation by the rapid expansion method (REM)—A one step time evolution algorithm: SEG Technical Program Expanded Abstracts, 2672–2676.

Tal-Ezer, H., D. Kosloff, and Z. Koren, 1987, An accurate scheme for seismic forward modelling: Geophysical Prospecting, **35**, 479–490.

Tessmer, E., 2011, Using the rapid expansion method for accurate time-stepping in modeling and reverse-time migration: Geophysics, **76**, no. 4, S177–S185.

Zhang, Y., J. Sun, and S. Gray, 2007, Reverse-time migration: Amplitude and implementation issues: SEG Technical Program Expanded Abstracts, 2145–2149.